ACS APPLIED MATERIALS & INTERFACES

Research Article

www.acsami.org

# Superior Properties of Silica Thin Films Prepared from Perhydropolysilazane Solutions at Room Temperature in Comparison with Conventional Alkoxide-Derived Silica Gel Films

Hiromitsu Kozuka,*[,†] Koji Nakajima,[‡] and Hiroaki Uchiyama[†]

[†]Faculty of Chemistry, Materials and Bioengineering, [‡]Graduate School of Science and Engineering, Kansai University, 3-3-35 Yamate-cho, Suita, 564-8680, Japan

Supporting Information

**ABSTRACT:** Preparation of silica thin films from perhydropolysilazane (PHPS) at room temperature has attracted much attention because it provides a new way to realize silica thin films in a variety of technologies where any high temperature processes should be avoided. Although silica gel films can also be prepared from alkoxides at room temperature by conventional sol-gel method, they are believed to have low mechanical and chemical durability. However, even such alkoxide-derived silica gel films have possibilities to become more durable via condensation reaction and densification when aged at room temperature. In order to clarify whether or not PHPS-derived silica thin films have critical superiority on properties, the hardness and chemical durability were compared between PHPS- and alkoxide-derived silica thin films, where PHPS films were exposed to the vapor from aqueous ammonia at room temperature for PHPS-to-silica conversion. Alkoxide-derived silica gel films were found to be densified and hardened when stored in air at room temperature, which resulted in pencil hardness even higher than 9H on Si(100) substrates. However, the ultra-microindentation tests demonstrated that the PHPS-derived films are definitely harder than the alkoxide-derived ones. The PHPS-derived films were also found to have higher chemical durability in water and in aqueous ammonia. Such higher mechanical and chemical durability of the PHPS-derived films was ascribed to their higher density, i.e., more highly condensed states, which was evidenced in infrared absorption spectra. Hard coating performance on plastic substrates was also studied, and the PHPS-derived films were demonstrated to have much higher adhesive strength on polymethylmethacrylate substrates. The in-plane stress measurement demonstrated that the PHPS-derived films have much lower or even negligible tensile stress, which may be one of the causes for such higher adhesive strength.

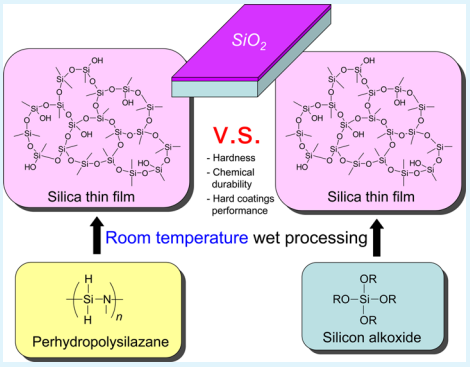


**KEYWORDS:** *silica, perhydropolysilazane, alkoxide, thin film, hard coatings, chemical durability*

## 1. INTRODUCTION

A solution-route utilizing perhydropolysilazane (PHPS), an inorganic polymer composed of Si−N skeletons with Si−H groups, as silica source has attracted much attention as a technique for preparing silica thin films. Such a PHPS-based solution route to silica thin films was first addressed by Matsuo et al., who deposited PHPS solutions on silicon wafers, followed by heat treatment at 450 °C.[1] They found that the PHPS-derived silica thin films have densities (2.1−2.2 g $cm^{-3}$), refractive indices (1.45−1.46), electrical resistivities (about $1 \times 10^{15}$ Ω cm) and dielectric constants (4.2) that are nearly identical to those of silica glass. Recently the authors' group has found that PHPS thin films can be converted into silica thin films at room temperature by an exposure to the vapor from aqueous ammonia.[2−6] The conversion of PHPS films into silica films has also been reported by Bauer et al., who exposed PHPS films in moisture-containing atmosphere in the presence of ammonia or amine as catalysts.[7] Since then, various techniques have been proposed for the conversion of PHPS films into silica films, including the standing in the ambient atmosphere,[8] the heat treatment in water vapor,[9] the exposure to vaporized ammonia atmosphere,[10] the reaction with water by the catalytic action of amine in the baking step,[11] the exposure to hydrogen peroxide vapor,[12] the hydrothermal treatment (for preparing phenylsilsesquioxane films),[13] the ultraviolet (UV) light irradiation,[14−16] the UV light irradiation under soaking in hydrogen peroxide,[17,18] and the $O_2$ plasma treatment followed by high-pressure $H_2O$ vapor heating.[19] Most of the processes are conducted near at room temperature, and involve water or its vapor, which indicates that the conversion may proceed via hydrolysis reaction.[20] This is the situation on the utilization of PHPS as the silica source, and the attention has grown rapidly.

The room-temperature processing is attractive when silica thin films are to be deposited on plastic substrates, for instance, as hard coatings. The authors previously reported that the silica films prepared by exposing PHPS films to the vapor from

Received: March 7, 2013
Accepted: July 31, 2013
Published: July 31, 2013

   dx.doi.org/10.1021/am400845y | ACS Appl. Mater. Interfaces 2013, 5, 8329−8336

aqueous ammonia have pencil hardness higher than 9H on silicon wafers,[5] and much higher durability in hot water than alkoxide-derived silica gel films.[2−5] However, alkoxide-derived silica gel films have possibilities to be densified and hardened when they are stored in air at room temperature because condenstation reaction would proceed. Then, it becomes unclear whether or not PHPS-derived silica films are definitely superior to alkoxide-derived silica gel films from the viewpoint of their mechanical and chemical durability. In addition, when such films are used as hard coatings on plastic substrates, the adhesion between the films and substrates becomes another issue to be focused on, and the comparison between PHPS- and alkoxide-derived films should be made on this issue.

To have clear knowledge on whether or not PHPS- and alkoxide-derived silica thin films have differences in mechanical properties and chemical durability, the comparison was made on the hardness, elastic modulus, and durability in acidic, neutral and basic aqueous solutions in the present study for silica thin films deposited on silicon substrates. The difference in structure was also studied on the basis of infrared (IR) absorption spectroscopy. To compare the hard coating performance between PHPS- and alkoxide-derived silica thin films, we also deposited the films on polymethylmethacrylate (PMMA) substrates, and the hardness and adhesion were measured and compared.

## 2. EXPERIMENTAL SECTION

**2.1. Sample Preparation.** For preparing PHPS-derived silica thin films, a xylene solution of PHPS (20%, NN110-20, AZ Electronic Materials, Tokyo, Japan) was used as the coating solution. The PHPS thin films were prepared by spin-coating at 750 - 8000 rpm on Si(100) substrates (20 mm × 40 mm × 0.52 mm). The as-deposited PHPS films were exposed to the vapor from aqueous ammonia at room temperature, where the films were kept standing vertically over 20 g 10 % aqueous ammonia using a glass support, where the lid of the bottle had three holes 5 mm in diameter so that the condensation of aqueous ammonia on the sample surface was avoided. For some of the samples, 24 h exposure treatment was followed by heat treatment at 1000 °C for 1 h in an electric furnace.

For preparing alkoxide-derived silica thin films, tetramethylorthosilicate ($Si(OCH_3)_4$, TMOS), tetraethylortosilicate ($Si(OC_2H_5)_4$, TEOS), 1 M nitric acid, methanol, ethanol, and ion-exchanged water were used as the starting materials. TEOS, nitric acid, methanol and ethanol were purchased from Wako Pure Chemical Industries (Osaka, Japan) and TMOS from Tokyo Chemical Industry Co. Ltd. (Tokyo, Japan). Starting solutions of mole ratios, $TMOS:H_2O:HNO_3:CH_3OH$ = 1:$x$:0.01:10 and $TEOS:H_2O:HNO_3:C_2H_5OH$ = 1:$x$:0.01:10, where $x$ = 2, 4, or 10, were prepared by the following procedure. A solution of water, nitric acid, and the half of the prescribed amount of alcohol was added under magnetic stirring to a solution consisting of alkoxide and the other half of the prescribed amount of alcohol. The solution thus obtained was stirred at room temperature for 1.5 h in a sealed glass container, and served as the coating solution while the TEOS solution of $x$ = 2 was stirred for 3 days. Spin-coating was conducted on Si(100) substrates (20 mm × 40 mm × 0.52 mm) at 1000−8000 rpm, and the resulting silica gel films were stored in the ambient atmosphere at room temperature for various periods of time.

For the in-plane residual stress measurements, the films were deposited on Si(100) wafers 0.51-0.53 mm in thickness and 100 mm in diameter. For evaluating hard coating performance, the films were deposited on polymethylmethacrylate (PMMA) substrates (20 mm × 40 mm × 3 mm). Some of the films were also deposited on 100 $\mu$m thick polyethyleneterephthalate (PET) sheets.

**2.2. Measurements and Observations.** The thickness of the films deposited on Si(100) substrates was measured by a contact probe surface profilometer (SE-3400, Kosaka Laboratory, Tokyo, Japan), a prism coupler with an He−Ne laser (2010, Metricon Corporation, New Jersey, U.S.A.) and an ellipsometer (ESM-1T, ULVAC, Chigasaki, Japan) with an He−Ne laser at an incident angle of 70°. For the measurement by the surface profilometer, a part of the films was scraped off with a surgical knife just after spin-coating, and the level difference thus created was measured after the exposure, storing in air or heat treatment. For some of the samples, the thickness was also evaluated from the cross-sectional images obtained by a scanning electron microscope (SEM) (JSM-6510, JEOL, Tokyo, Japan).

The IR absorption spectra of the films on Si(100) substrates were measured using a Fourier transform IR spectrometer (FT/IR-410, Jasco, Tokyo, Japan), where a bare Si(100) substrate was used as the reference.

The pencil hardness of the films on Si(100) substrates was measured using a pencil hardness tester (553-M1, Yasuda Seiki, Nishinomiya, Japan) where 750 g load was applied on the sample. The hardness was tested on a 3 mm line on five different locations, and the pencil hardness that left scratches on less than two lines was defined as the hardness of the sample.

The ultra-microindentation tests were performed on the films deposited on Si(100) substrates using a dynamic ultramicrohardness tester (DUH-W201S, Simadzu Corporation, Kyoto, Japan) with a diamond trigonal pyramid indenter of an angle of 115° between two edges. The load−displacement curves were obtained at a loading rate of 1.422 mN/s with a hold period duration of 5 s at the maximum load of 1−8 mN. A typical load ($P$)−displacement ($h$) curve is given in Figure 1, where some of the experimental quantities are defined,

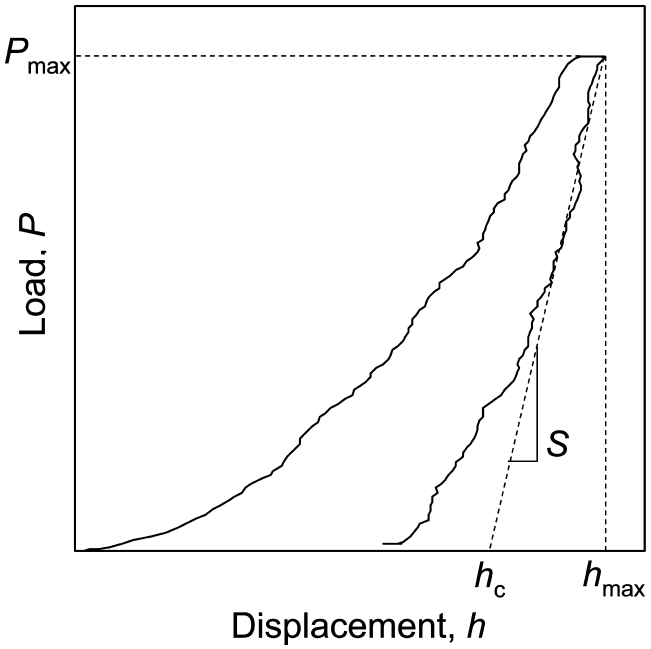


**Figure 1.** Typical load ($P$)−displacement ($h$) curve obtained by the ultra-microindentation test, and the definition of the maximum load, $P_{max}$, displacement at the maximum load, $h_{max}$, the slope of the initial portion of the unloading curve, $S$ = d$P$/d$h$, and contact depth, $h_c$.

including the maximum load, $P_{max}$ (N), the displacement at the maximum load, $h_{max}$ ($\mu$m), the slope of the initial portion of the unloading curve (intinial stiffness), $S$ = d$P$/d$h$ (N/$\mu$m), and contact depth, $h_c$. Dynamic hardness $H_D$ was calculated by the following equation:

$$H_D = 3.8584 P_{max}/{h_{max}}^2 \quad (1)$$

where 3.8584 is a geometrical constant of the indenter. Elastic modulus, $Y$, was obtained by the following equations:

$$Y = \frac{E}{1-\nu^2} \quad (2)$$

$$\frac{1}{E_r} = \frac{1-\nu^2}{E}\frac{1-\nu_i^2}{E_i} \quad (3)$$

$$E_r = \frac{S}{2h_c}\sqrt{\frac{\pi}{23.97}} \quad (4)$$

where $E$ and $\nu$ are the Young's modulus and Poisson's ratio of the sample, and $E_i$ and $\nu_i$ the same parameters of the indenter, where $E_i$ = 1140 GPa and $\nu_i$ = 0.07, $E_r$ the reduced modulus, and 23.97 the constant for the indenter.

Cross-cut tape test was conducted for the films deposited on PMMA substrates. One-hundred-sectioned grid (10 × 10 sections), with meshes 1 mm × 1 mm in size, was made using a cross-cut guide (CCJ-1, Cotec Corporation, Tokyo, Japan) and a utility knife. A pressure-sensitive adhesive tape (CT-15, Nichiban Co., Ltd., Tokyo, Japan) was stuck on the grid and rubbed by a finger so as to adhere the tape completely on the film, then sharply removed vertical to the surface. The grid was observed using an optical microscope (KH-1300, Hirox Co., Ltd., Tokyo, Japan), and the fraction of the meshes that underwent delamination was evaluated. Even when a mesh has only partial delamination, such a mesh was counted as a delaminated one.

Chemical durability of the films deposited on Si(100) substrates was evaluated by immersing them in aqueous test solutions. The sample was kept standing vertically in test solutions using a glass holder in all cases. The test solutions were water (80 °C, 100 g), 36.5 % aqueous hydrochloric acid (25 °C, 50 g), and 1 M and 10% aqueous ammonia (25 °C, 50 g). The water was kept in a sealed glass container, and the acidic and basic solutions in sealed polypropylene containers.

## 3. RESULTS

**3.1. Changes in Structure and Properties Observed during the Exposure Treatment and Storing in Air.** The changes in IR absorption spectra during the exposure treatment were studied for the PHPS-derived films deposited on Si(100) substrates at 1500 rpm. As seen in Figure 2**a** the as-deposited PHPS film had absorption peaks at 3375 ($\nu_{N-H}$), 2162 ($\nu_{Si-H}$), 1180 ($\delta_{N-H}$), 920 ($\nu_{asymmetric,\ Si-N}$ in Si−N−Si), and 840 $cm^{-1}$ ($\nu_{asymmetric,\ Si-N}$ in Si−N−Si), where $\nu$ and $\delta$ denote the stretching and bending vibrations, respectively, and the assignments were made after ref 21. The film also had small absorption peaks at 1100 (LO mode of $\nu_{asymmetric,\ Si-O-Si}$) and 1010 $cm^{-1}$ (TO mode of $\nu_{asymmetric,\ Si-O-Si}$).[22] When the exposure time was increased from 2 to 3 h, the PHPS film was converted into a silica film containing Si−OH and Si−H groups, which is evidenced in the following changes in the IR absorption spectra. The 3375 $cm^{-1}$ peak ($\nu_{N-H}$) disappeared, whereas a broad band at 3350 $cm^{-1}$ with a peak at 3650 $cm^{-1}$ appeared; the former is assigned to $\nu_{O-H}$ and the latter to mutually hydrogen bonded SiO-H or internal SiO-H stretching vibrations.[23] The bands at 1180 ($\delta_{N-H}$), 920 ($\nu_{asymmetric,\ Si-N}$ in Si−N−Si) and 840 $cm^{-1}$ ($\nu_{asymmetric,\ Si-N}$ in Si−N−Si) disappeared while a band grew at 1060 $cm^{-1}$ (TO mode of $\nu_{asymmetric,\ Si-O-Si}$) with a shoulder at 1170 $cm^{-1}$ (LO mode of $\nu_{asymmetric,\ Si-O-Si}$). New bands appeared at 940 ($\nu_{Si-OH}$), 800 ($\nu_{symmetric,\ Si-O-Si}$) and 450 $cm^{-1}$ ($\rho_{Si-O-Si}$), where $\rho$ denotes rocking vibration. A small peak emerged at 880 $cm^{-1}$, which is assigned to $\omega_{Si-H}$ (wagging vibration).[24] The band at 2162 $cm^{-1}$ diminished and a small band at 2250 $cm^{-1}$ emerged, both of which are assigned to $\nu_{Si-H}$ because Si−H stretching vibration is known to appear at 2100−2200 and 2250 $cm^{-1}$, respectively, when the Si atom is bonded with nitrogen and oxygen atoms.[24−26] During such PHPS-to-silica conversion, especially at exposure time of 2−3 h, the pencil hardness increased as seen in Table 1.

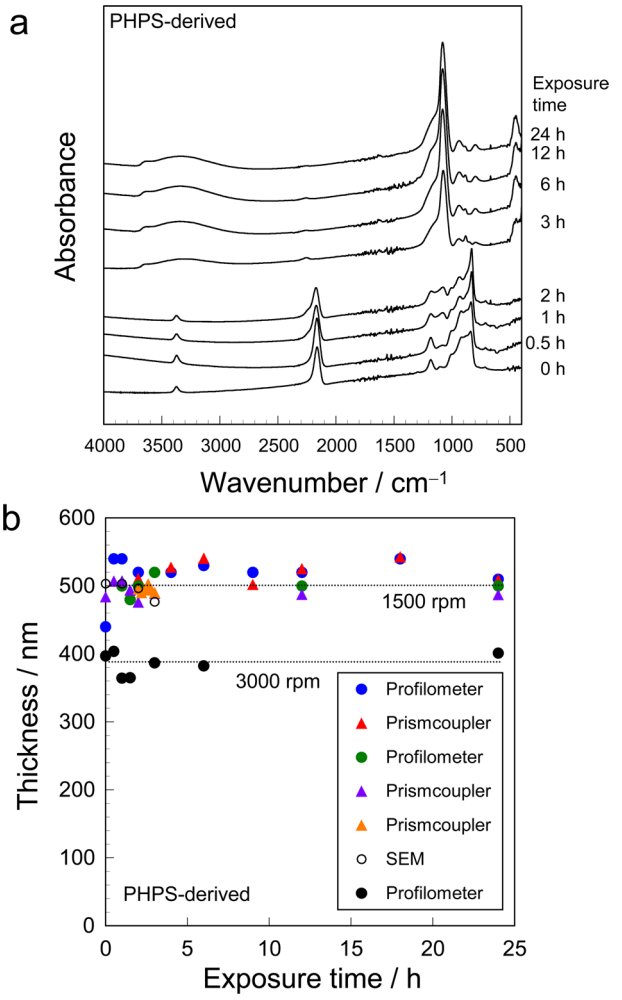


**Figure 2.** (a) IR absorption spectra and (b) thickness of the PHPS-derived films exposed to the vapor from the aqueous ammonia for various periods of time. The films were prepared at (a) 1500 rpm and (b) 1500 and 3000 rpm. The thickness was measured with the profilometer, prismcoupler and ellipsometer as well as via SEM cross-section observation as denoted in b.

**Table 1. Pencil Hardness of the PHPS-Derived Films Deposited on Si(100) Substrates at 1500 rpm and Exposed to the Vapor from Aqueous Ammonia for Various Periods of Time**

| exposure time (h) | pencil hardness |
|---|---|
| 0 | <6B |
| 1 | <6B |
| 1.5 | 5B |
| 2 | 3H |
| 3 | 8H |
| 12 | 9H |
| 24 | >9H |

The variation of thickness during the exposure treatment was also studied for these PHPS-derived films as well as those deposited at 3000 rpm. The sample preparation was performed several times, and the measurement was conducted using various techniques as denoted in Figure 2b. As seen in the figure, the film thickness was almost unchanged during the PHPS-to-silica conversion. Even after being stored in air for 60 days after the exposure treatment, the film prepared at 1500

rpm had almost similar thickness of 483 nm, which indicates that PHPS-derived silica films do not undergo further densification during storing in air.

The changes in IR absorption spectra during storing in air were studied for the TMOS-derived films that were prepared from a solution of an $H_2O$/TMOS mole ratio ($x$) = 4 on Si(100) substrates at 1500 rpm (Figure 3a). The spectra had a broad band at 3350 $cm^{-1}$ ($\nu_{O-H}$) with a peak at 3650 $cm^{-1}$ ($\nu_{SiO-H}$), a band at 1060 $cm^{-1}$ (TO mode of $\nu_{asymmetric,\ Si-O-Si}$) with a shoulder at 1170 $cm^{-1}$ (LO mode of $\nu_{asymmetric,\ Si-O-Si}$), and peaks at 940 ($\nu_{Si-OH}$), 800 ($\nu_{symmetric,\ Si-O-Si}$) and 450 $cm^{-1}$ ($\rho_{Si-O-Si}$). When the film was stored in air for longer periods of time, the 940 ($\nu_{Si-OH}$) and 3350 $cm^{-1}$ ($\nu_{O-H}$) bands slightly decreased, suggesting the progress of condensation reaction in the film. Such changes are more clearly seen in Figure 3b, where the $\nu_{Si-OH}/\nu_{asymmetric,\ Si-O-Si}$ and $\nu_{O-H}/\nu_{asymmetric,\ Si-O-Si}$ peak area ratios are plotted versus storing time. The progress of condensation reaction resulted in a reduction in thickness as is seen in Figure 3c, where the thickness of the TMOS-derived film is plotted versus storing time. Such progress of condensation was followed by an increase in pencil hardness as seen in Table 2, where the pencil hardness is shown as a function of storing time for TMOS- and TEOS-derived films prepared at 1500 rpm on Si(100) substrates. The hardness even reached over 9H when the films were stored in air.

The variation of in-plane stress during storing in air was studied for the PHPS- and TMOS-derived ($x$ = 4) films that were deposited on Si(100) wafers at 1500 rpm. The PHPS- and TMOS-derived films were stored in air after 24 h exposure treatment and after deposition, respectively. As seen in Figure 4, the TMOS-derived film had tensile, in-plane stress, which increased with increasing storing time, i.e. with the progress of condensation reaction. On the other hand, the stress was almost negligible and unchanged with increasing storing time for the PHPS-derived film.

### 3.2. Comparison of Hardness, Chemical Durability, and Structure between PHPS- and TMOS-Derived Films.

As clarified in the above section, the TMOS-derived silica gel films harden when stored in air at room temperature, where the condensation reaction proceeds and the films are densified. Therefore, it is now unclear if PHPS-derived silica thin films truly have superiority on hardness as well as chemical durability compared with such TMOS-derived, aged thin films. Then hardness and chemical durability as well as structure were compared between the PHPS- and TMOS-derived films, the latter of which were stored in air for a long period of time.

Panels a and b in Figure 5 show the dynamic hardness and elastic modulus, respectively, measured using the dynamic ultramicrohardness tester on the PHPS- and TMOS-derived films deposited on Si(100) substrates. A 780-nm-thick PHPS-derived film was prepared at 750 rpm and exposed for 24 h, whereas a 829-nm-thick TMOS-derived one was prepared by twice depositions at 1500 rpm. The TMOS-derived film was stored in air for 144 h after deposition; in other words, the film was hardened by the storing. As seen in the figures the PHPS-derived film had higher hardness and elastic modulus than the TMOS-derived one, irrespective of the penetration depth.

The chemical durability was also compared for the PHPS- and TMOS-derived ($x$ = 4) films. First the durability in 80 °C water was evaluated by measuring the thickness with the contact probe surface profilometer after soaking for various periods of time. Both films were prepared at 1500 rpm, where the PHPS-derived films were exposed for 24 h, and the TMOS-derived films were stored in air for 72 and 144 h before soaking. As seen in Figure 6a, the reduction in thickness by soaking was negligible for the PHPS-derived film, whereas the TMOS film stored in air for 72 h exhibited significant reduction in thickness, where the thickness became negligible at a soaking

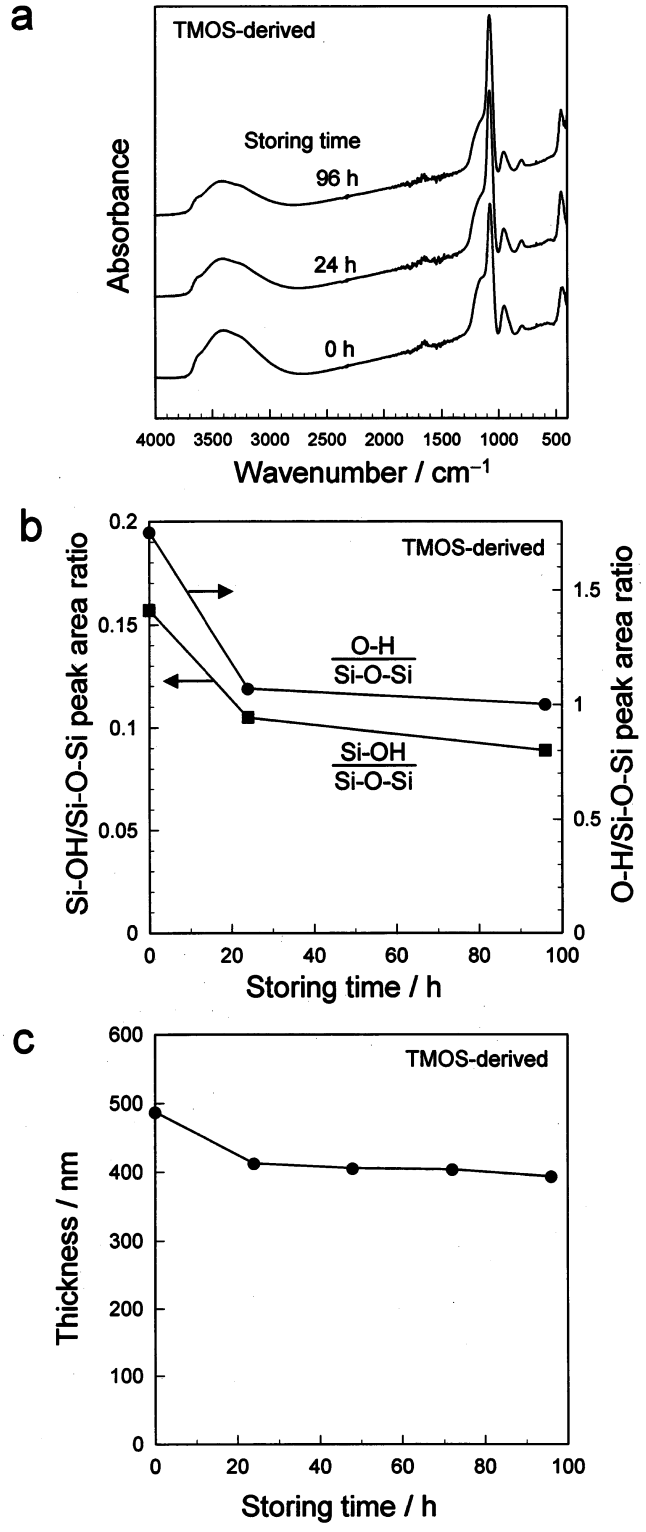


**Figure 3.** (a) IR absorption spectra, (b) $\nu_{Si-OH}/\nu_{asymmetric,\ Si-O-Si}$ and $\nu_{O-H}/\nu_{asymmetric,\ Si-O-Si}$ peak area ratios, and (c) thickness of the TMOS-derived films that were prepared from a solution of $x$ = 4 on Si(100) substrates at 1500 rpm, followed by storing in air for various periods of time.


dx.doi.org/10.1021/am400845y | ACS Appl. Mater. Interfaces 2013, 5, 8329−8336

**Table 2. Pencil Hardness of the TMOS- and TEOS-Derived Films Deposited on Si(100) Substrates at 1500 rpm and Stored in Air for Various Periods of Time[a]**

| | | pencil hardness | | | | |
|---|---|---|---|---|---|---|
| alkoxide | $H_2O$/alkoxide mole ratio, $x$ | <1 h | 3 h | 24 h | 48 h | 72 h |
| TMOS | 2 | 4H | >9H | 9H | >9H | >9H |
| TMOS | 4 | 3H | 4H | 4H | >9H | >9H |
| TMOS | 10 | 4H | 8H | >9H | >9H | >9H |
| TEOS | 2 | <6B | F | 4H | 5H | 6H |
| TEOS | 4 | 4H | >9H | >9H | >9H | >9H |
| TEOS | 10 | 6H | >9H | >9H | >9H | >9H |

[a]The times in the table denote the storing time.

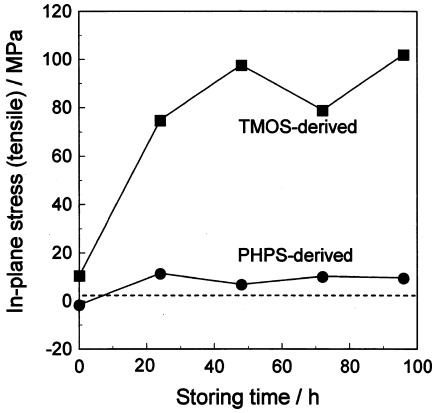


**Figure 4.** In-plane stress as a function of the time for storing in the ambient atmosphere for the PHPS- and TMOS-derived ($x$ = 4) films that were deposited on Si(100) wafers at 1500 rpm. The PHPS- and TMOS-derived films were kept standing in the ambient atmosphere for various periods of time after the 24 h exposure treatment and after deposition, respectively.

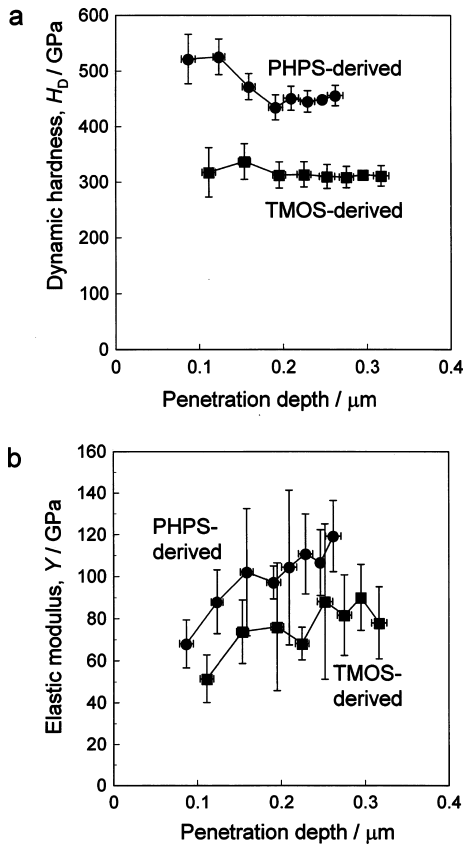


**Figure 5.** (a) Dynamic hardness and (b) elastic modulus of the PHPS- and TMOS-derived films deposited on Si(100) substrates. The PHPS-derived film was prepared at 750 rpm, exposed for 24 h, and 780 nm in thickness, whereas the TMOS-derived one was deposited at 1500 rpm, which was repeated twice, and was 829 nm in thickness. The TMOS-derived film was stored in the ambient atmosphere for 144 h after deposition.

time over 13 h. When stored in air for a longer period of 144 h, the TMOS-derived film showed less reduction in thickness, which, however, was still significant. To clarify whether or not the reduction in thickness truly resulted from film dissolution, the IR absorption spectra were measured on the films after soaking, which are shown in Figure S1a, b in the Supporting Information. The PHPS-derived films showed no change in spectra while the TMOS-derived one stored in air for 72 h had no absorption bands when soaked over 13 h. Therefore, the thickness reduction occurring during soaking surely resulted from the film dissolution.

The durability in acidic and basic solutions was also studied by similar assessment. In 36% hydrochloric acid, both PHPS- and TMOS-derived films exhibited no reduction in thickness, showing high durability (Figure 6b). In 1M and 10% (5.6 M) aqueous ammonia, on the other hand, where the thickness was measured by the ellipsometer, the PHPS-derived film showed negligible changes in thickness, whereas the TMOS-derived films exhibited reduction, indicating less chemical durability (Figures 6c). Such changes in thickness surely resulted from the film dissolution, which are supported by the IR absorption spectra measured after soaking. As seen in Figure S2a, b in the Supporting Information, the PHPS-derived film showed negligible changes in spectra, whereas the TMOS-derived films exhibited reduction in absorption bands.

To compare the concentration of Si−O−Si and OH groups between the PHPS- and TMOS-derived films, the IR absorption peak area per film thickness was obtained for the bands at 1000−1200 $cm^{-1}$ ($\nu_{\text{asymmetric Si−O−Si}}$) and 3000−3700 $cm^{-1}$ ($\nu_{\text{O−H}}$) via peak deconvolution. Table 3 shows the $\nu_{\text{asymmetric Si−O−Si}}$, $\nu_{\text{O−H}}$, and $\nu_{\text{Si−OH}}$ peak area per thickness obtained for the PHPS- and the TMOS-derived ($x$ = 4) films prepared at 1500 rpm, the latter of which was stored in air for 144 h. It is seen that the PHPS-derived film has larger $\nu_{\text{asymmetric Si−O−Si}}$ and smaller $\nu_{\text{O−H}}$ and $\nu_{\text{Si−OH}}$ peak area per thickness, indicating the higher Si−O−Si, and lower OH and Si−OH concentrations. To obtain further information on the difference in density, the PHPS- and TMOS-derived films were fired at 1000 °C for 1 h, and the reduction in thickness was compared. Both films were prepared at 1500 rpm, and the TMOS-derived film was stored in air for 18 days before firing. The PHPS-derived film showed a 29% reduction in thickness, whereas the TMOS-derived one showed a slightly larger reduction of 34%, suggesting the higher density of the PHPS-derived film in unfired state than the TMOS-derived one.

**3.3. Hard Coating Performance.** Hard coating performance was compared between the PHPS- and TMOS-derived films that were deposited on PMMA substrates. Table 4 shows the pencil hardness of the PHPS- and TMOS-derived films deposited on PMMA substrates at various spinning rates where the PHPS-derived films were exposed for 24 h, the TMOS-derived films were stored in air for 72 h, and the thickness was measured on films deposited on Si(100) substrates. All the


dx.doi.org/10.1021/am400845y | ACS Appl. Mater. Interfaces 2013, 5, 8329−8336

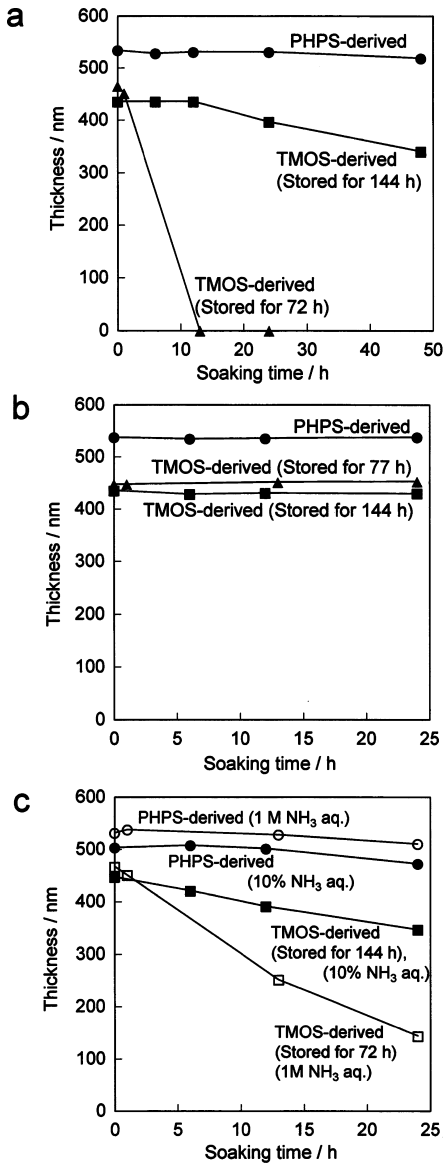


**Figure 6.** Thickness of the PHPS- and TMOS-derived ($x$ = 4) films measured after soaking (a) in 80 °C water, (b) in 36% hydrochloric acid, and (c) in 1M and 10% aqueous ammonia for various periods of time. Both films were prepared at 1500 rpm, where the PHPS-derived films were exposed for 24 h and the TMOS-derived films were stored in air for 72 and 144 h before soaking. The thickness was measured by the contact probe surface profilometer for (a) and (b) and by the ellipsometer for (c).

**Table 3. Band Area Per Thickness for $\nu_{Si-O-Si}$, $\nu_{O-H}$, and $\nu_{Si-OH}$ Bands Obtained for the PHPS- and TMOS-Derived Films Prepared on Si(100) Substrates at 1500 rpm[a]**

| | | band area per thickness ($cm^{-1}$ $\mu m^{-1}$) | | |
|---|---|---|---|---|
| silica source | thickness (nm) | $\nu_{Si-O-Si}$ | $\nu_{O-H}$ | $\nu_{Si-OH}$ |
| PHPS | 504 | 98.5 | 65.2 | 7.9 |
| TMOS | 436 | 83.4 | 73.8 | 8.5 |

[a]The TMOS-derived film was stored in air for 144 h.

films had pencil hardness of 3H−4H, showing no significant difference irrespective of the silica source and of the thickness. However, significant difference was detected on the scratches made by the pencil hardness tests as seen in Figure 7, where the

**Table 4. Pencil Hardness and Delamination Fraction on the Cross-Cut Tape Test for the PHPS- and TMOS-Derived Films Deposited on PMMA Substrates at Various Spinning Rates[a]**

| silica source | spinning rate (rpm) | thickness (nm) (on Si(100)) | pencil hardness (on PMMA) | delamination fraction (%) (on PMMA) |
|---|---|---|---|---|
| PHPS | 1000 | 610 | 3H | 0 |
| PHPS | 2000 | 430 | 4H | 0 |
| PHPS | 4000 | 280 | 3H | 0 |
| PHPS | 6000 | 240 | 4H | 0 |
| PHPS | 8000 | 200 | 3H | 0 |
| TMOS | 1000 | 540 | 3H | 100 |
| TMOS | 2000 | 340 | 3H | 100 |
| TMOS | 4000 | 240 | 3H | 100 |
| TMOS | 6000 | 220 | 4H | 100 |
| TMOS | 8000 | 200 | 3H | 100 |

[a]The TMOS-derived films were stored in air for 72 h. The thickness of the films were measured on those deposited on Si(100) substrates.

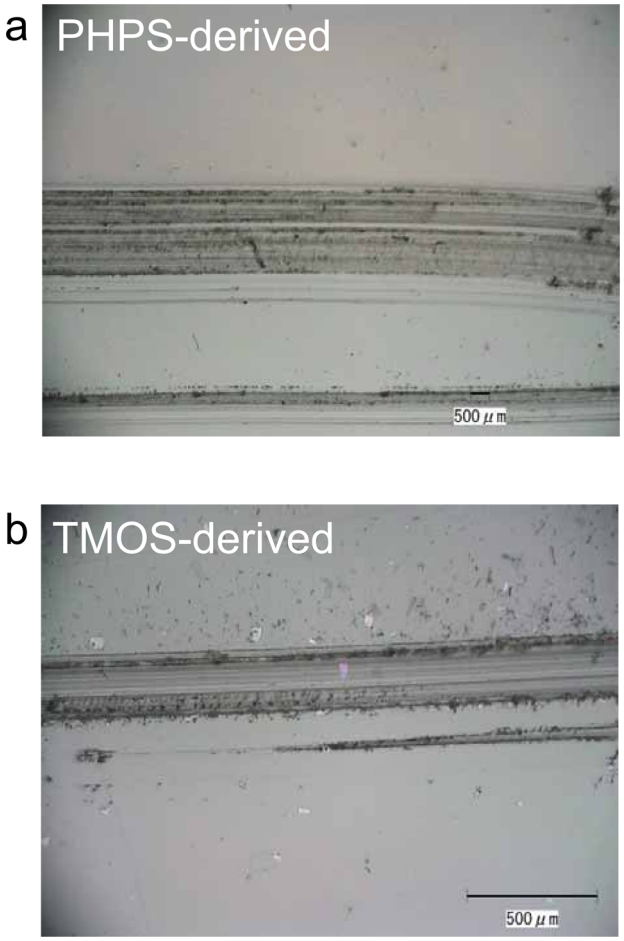


**Figure 7.** Scratches made by a pencil of 10H under a load of 750 g on the (a) PHPS- and (b) TMOS-derived films that were prepared at 1000 rpm on PMMA substrates. The PHPS films were exposed for 24 h, and the TMOS-derived films were stored in air for 72 h.

scratches were made by a pencil of 10H under a load of 750 g on the PHPS- and TMOS-derived films that were prepared at 1000 rpm on PMMA substrates. Fragments of the film were seen for the TMOS-derived film (Figure 7b), wheras no such fragments were detected for the PHPS-derived one (Figure 7a).


dx.doi.org/10.1021/am400845y | ACS Appl. Mater. Interfaces 2013, 5, 8329−8336

This suggests larger interfacial adhesive strength for the PHPS-derived films, which is more clearly revealed in the optical micrographs taken after the cross-cut tape test for the PHPS- and TMOS-derived ($x$ = 4) films deposited at 1000 rpm on PMMA substrates (Figure 8). Even partial delamination was

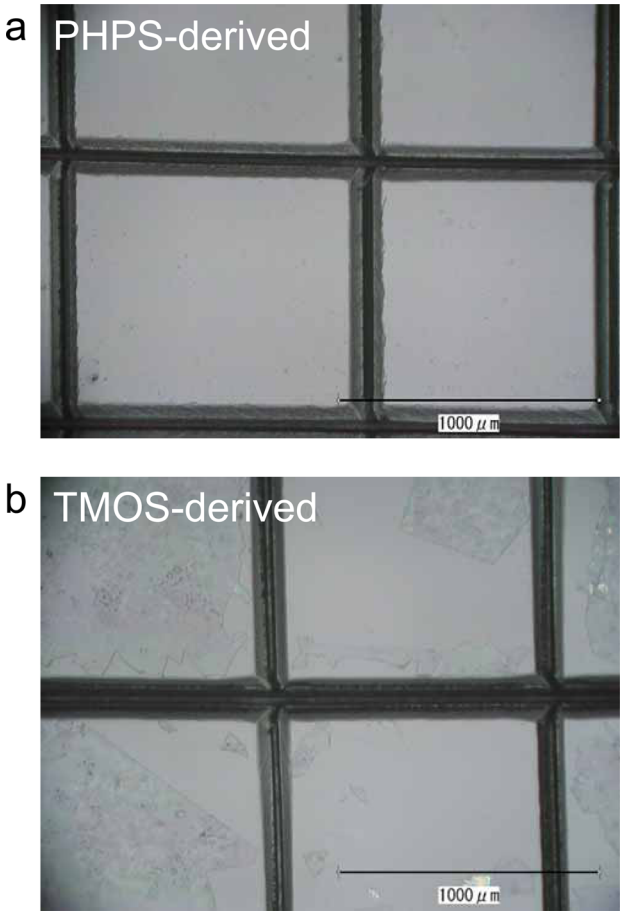


**Figure 8.** Optical micrographs of the (a) PHPS- and (b) TMOS-derived ($x$ = 4) films on PMMA substrates taken after the cross-cut tape test. The films were prepared at 1000 rpm, where the PHPS-derived film was exposed for 24 h, and the TMOS-derived film was stored in air for 72 h.

detected in none of the meshes for the PHPS-derived film while partial delaminatation was detected in every mesh for the TMOS-derived film. As described in the Experimental Section, even when a mesh has only partial delamination, such a mesh was counted as a delaminated one. On the basis of such criteria, the delamination fraction was evaluated to be 0 and 100% for the PHPS- and TMOS-derived films, respectively, as shown in Table 4.

A 100 $\mu$m thick PET sheet was coated with the PHPS- (exposed for 24 h) and TMOS-derived ($x$ = 4) films at 1500 rpm, and after storing in air for 8 days, the bending of the sheet was observed. As seen in Figure 9, the sheet with the PHPS-derived film showed no bending while that with the TMOS-derived film was bent concavely on the coated side.

## 4. DISCUSSION

The TMOS-derived silica films underwent condensation reaction during storing in air (Figure 3b), and as a result they were densified and hardened; the densification and

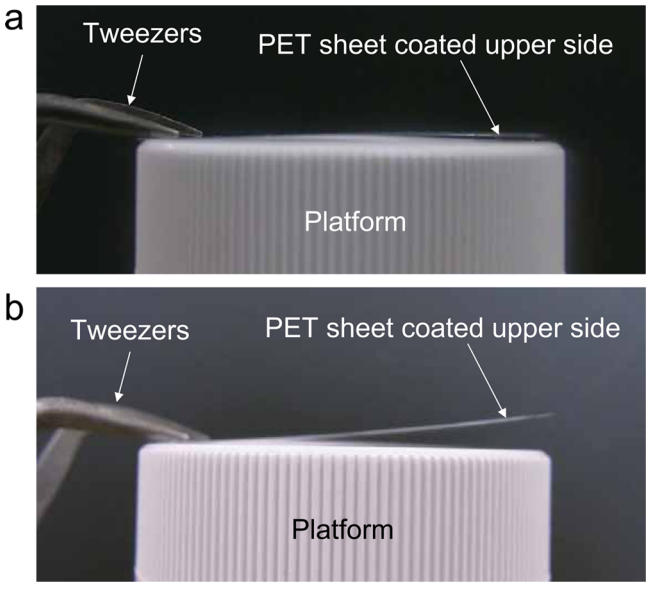


**Figure 9.** Demonstration of the bending of a 100 $\mu$m thick PET sheet, one side of which was coated with the (a) PHPS- and (b) TMOS-derived ($x$ = 4) films at 1500 rpm. The PHPS-derived film was exposed for 24 h. The photographs were taken 8 days after deposition.

hardening were evidenced in the reduction in thickness (Figure 3c) and in the increase in pencil hardness (Table 1), respectively. Durability in water and in aqueous ammonia was also enhanced when the TMOS-derived silica films were stored in air for longer periods of time (Figure 6a, c).

However, even compared with the TMOS-derived silica films that were stored in air for long periods, the PHPS-derived silica films possessed higher hardness, elastic moduli (Figure 5) and chemical durability (Figure 6a, c) than the TMOS-derived ones. Such higher mechanical and chemical resistances of the PHPS-derived films are ascribed to their more highly densified states, i.e. more condensed states, which is evidenced in the higher Si−O−Si and lower OH and Si−OH concentrations in the PHPS-derived films (Table 3) as well as in the smaller reduction in thickness observed on firing at 1000 °C. As far as the chemical durability is concerned, it is known that the rate of dissolution of silica increases with increasing pH over 2, and the dissolution occurs via nucleophilic attack on silicon atoms by $OH^-$ ions.[27] The PHPS-derived silica films have more condensed states with less amounts of silanol groups, which retards the diffusion of $OH^-$ ions in films and also precludes silicate monomers from being released from films. This illustrates the higher durability of the PHPS-derived films in water and in aqueous ammonia. Considering the negligible reduction in thickness during the exposure treatment (Figure 2b), the as-deposited PHPS films may already be in densified states. Why PHPS-derived silica films have more highly condensed states than TMOS-derived ones, and why such highly condensed states are achieved in PHPS-derived silica films are issues to be answered, and should be studied in near future.

As far as the hard coating performance is concerned, the pencil hardness on PMMA substrates (Table 4) was much lower than that on Si(100) substrates (Tables 1 and 2) for both PHPS- and TMOS-derived films. This is just because of the much lower hardness of the underlying PMMA substrates, which undergoes depression under the pencil load, leading to the fracture of the silica overlayers. The significant difference between the PHPS- and TMOS-derived coatings was the much


dx.doi.org/10.1021/am400845y | ACS Appl. Mater. Interfaces 2013, 5, 8329−8336

higher adhesive strength on PMMA substrates for the PHPS-derived ones (Table 4 and Figure 8). This could be attributed to a smaller amounts of silanol groups for the PHPS-derived films than the TMOS-derived ones (Table 3), which makes the PHPS-derived films more hydrophobic, leading to their higher affinity to the hodrophobic PMMA substrate surface. The presence of a trace amount of Si−H and Si−N groups at the contact surface of the PHPS-derived films could also contribute, but to much less extent, to van der Waals interaction with the hydrophobic PMMA substrate surface. Another factor that could contribute to the larger adhesive strength is the lower in-plane stress in the PHPS-derived films, which was evidenced in Figure 4 as well as in the absence of the bending on the PET sheet (Figure 9). The higher in-plane stress in the TMOS-derived films may assist the delamination, and such a factor is absent in the PHPS-derived ones. The tensile stress results from the shrinkage of the film that is constrained on the substrate surface.[28] The TMOS-derived films undergo shrinkage because of the progress of condensation reaction during storing in air, whereas the PHPS-derived film do not, which is the reason for the difference in stress evolution.

## 5. CONCLUSIONS

Silica gel films prepared from TMOS solutions were shown to be densified via the progress of condensation reaction and to be hardened when stored in air at room temperature, which resulted in pencil hardness even higher than 9H on Si(100) substrates. However, the ultra-microindentation tests demonstrated that PHPS-derived films are harder than the TMOS-derived ones. The PHPS-derived films were also shown to have higher chemical durability in water and in aqueous ammonia. Such higher mechanical and chemical durability of the PHPS-derived films were ascribed to their higher density, i.e., more highly condensed states than those of the TMOS-derived films. In spite of similar pencil hardness on PMMA substrates, which was due to the small film thickness and the softness of PMMA, the PHPS-derived films exhibited much higher adhesive strength on PMMA substrates, which is a great advantage for hard coatings. The much smaller or even negligible in-plane, tensile stress in the PHPS-derived films compared with the TMOS-derived ones, which was demonstrated by the stress measurement, could be one of the causes for such higher adhesive strength.

## ■ ASSOCIATED CONTENT

### Supporting Information

IR spectra of the PHPS- and TMOS-derived films measured after soaking in 80 °C water (Figure S1) and in 1M and 10% aqueous ammonia (Figure S2) for various periods of time. This material is available free of charge via the Internet at http://pubs.acs.org.

## ■ AUTHOR INFORMATION

### Corresponding Author

*E-mail: kozuka@kansai-u.ac.jp.

### Notes

The authors declare no competing financial interest.

## ■ ACKNOWLEDGMENTS

This work was supported by (i) Suzuki Foundation Grant-in-Aid, 2010-2011, (ii) JSPS Grant-in-Aid for Exploratory Research, 2011-2012, and (iii) High-Tech Research Center Project for Private Universities: Matching Fund Subsidy from MEXT, 2007-2011.

## ■ REFERENCES

(1) Matsuo, H.; Yamada, K. *Convertech* **1995**, *23*, 25−29 [in Japanese].
(2) Kubo, T.; Tadaoka, E.; Kozuka, H. *J. Mater. Res.* **2004**, *19*, 635−642.
(3) Kubo, T.; Tadaoka, E.; Kozuka, H. *J. Sol−Gel Sci. Technol.* **2004**, *31*, 257−261.
(4) Kubo, T.; Kozuka, H. *J. Ceram. Soc. Jpn.* **2006**, *114*, 517−523.
(5) Kozuka, H.; Fujita, M.; Tamoto, S. *J. Sol−Gel Sci. Technol.* **2008**, *48*, 148−155.
(6) Yamano, A.; Kozuka, H. *J. Phys. Chem. B* **2009**, *113*, 5769−5776.
(7) Bauer, F.; Decker, U.; Dierdorf, A.; Ernst, H.; Heller, R.; Liebe, H.; Mehnert, R. *Prog. Org. Coatings* **2005**, *53*, 183−190.
(8) Kinashi, K.; Nakamura, S.; Ono, Y.; Ishida, K.; Ueda, Y. *J. Photochem. Photobiol. A - Chem.* **2010**, *213*, 136−140.
(9) Lee, H. S.; Park, K.; Kim, J. D.; Han, T.; Ryu, K. H.; Lim, H. S.; Lee, D. R.; Kwark, Y. J.; Cho, J. H. *J. Mater. Chem.* **2011**, *21*, 6968−6974.
(10) Fang, Q. L.; Kim, D. P.; Li, X. D.; Yoon, T. H.; Li, Y. H. *Lab Chip* **2011**, *11*, 2779−2784.
(11) Terai, M.; Ishibashi, T.; Shinohara, M.; Yonekura, K.; Hagiwara, T.; Hanawa, T.; Kumada, T. *Proc. SPIE* **2008**, *6924*, 92420−92420.
(12) Tanaka, K.; Hanaoka, K.; Yamaguchi, M.; Shindo, T.; Kunzelmann, K. H.; Teranaka, T. *Dental Mater. J.* **2011**, *30*, 170−175.
(13) Imanari, N.; Sugahara, Y. *Sci. Adv. Mater.* **2010**, *2*, 195−199.
(14) Naganuma, Y.; Tanaka, S.; Kato, C.; Shindo, T. *J. Ceram. Soc. Jpn.* **2004**, *112*, 599−603.
(15) Prager, L.; Dierdorf, A.; Liebe, H.; Naumov, S.; Stojanovic, S.; Heller, R.; Wennrich, L.; Buchmeiser, M. R. *Chem.—Eur. J.* **2007**, *13*, 8522−8529.
(16) Scherzer, T.; Mirschel, G.; Heymann, K.; Prager, L.; Buchmeiser, M. R. *Appl. Spectrosc.* **2009**, *63*, 239−245.
(17) Jung, S. H.; Lee, J. S.; Oh, J. H.; Moon, S. W.; Kim, S. D. *Jpn. J. Appl. Phys.* **2010**, *49*, 111505.
(18) Lee, J. S.; Oh, J. H.; Moon, S. W.; Sul, W. S.; Kim, S. D. *Electrochem. Solid-State Lett.* **2010**, *13*, II23−II25.
(19) Urabe, Y.; Sameshima, T. *Mater. Res. Soc. Symp. Proc.* **2008**, *1066*, 107−111.
(20) Dargère, N.; Bounor-Legaré, V.; Boisson, F.; Cassagnau, P.; Martin, G.; Sonntag, P.; Garois, N. *J. Sol−Gel Sci. Technol.* **2012**, *62*, 389−396.
(21) Trasferetti, B. C.; Gelamo, R. V.; Rouxinol, F. P.; Bica de Moraes, M. A.; Davanzo, C. U. *Chem. Mater.* **2005**, *17*, 4685−4692.
(22) Almeida, R. M.; Pantano, C. G. *J. Appl. Phys.* **1990**, *68*, 4225−4262.
(23) Brinker, C. J.; Scherer, G. W. *Sol−Gel Science, The Physics and Chemistry of Sol−Gel Processing*; Academic Press: New York, 1990; Chapter 9.
(24) Nakajima, K.; Uchiyama, H.; Kitano, T.; Kozuka, H. *J. Am. Ceram. Soc.*, in press.
(25) Tsu, D. V.; Lucovsky, G.; Mantini, M. J. *Phys. Rev. B* **1986**, *33*, 7069−7076.
(26) Lucovsky, G. *J. Non-Cryst. Solids* **1998**, *227*, 1−14.
(27) Brinker, C. J.; Scherer, G. W. *Sol−Gel Science, The Physics and Chemistry of Sol−Gel Processing*; Academic Press: New York, 1990; Chapter 3.
(28) Kozuka, H. *J. Sol−Gel Sci. Technol.* **2006**, *40*, 287−297.